Progress In Electromagnetics Research, PIER 97, 1–10, 2009

TUNABLE PERIODIC MICROSTRIP STRUCTURE ON GAAS WAFER

L. Matekovits †

Dipartimento di Elettronica
Politecnico di Torino
C.so Duca degli Abruzzi, 24, Torino 10129, Italy

M. Heimlich and K. Esselle

Department of Electronic Engineering
Macquarie University
Sydney, NSW 2109, Australia

Abstract—A one dimensional tunable periodic structure in microstip technology on gallium arsenide (GaAs) substrate is numerically investigated. The unit cell contains a number of patches positioned between the ground plane and the microstrip line. The patches, representing reactive loads, can be selectively short-circuited by externally-controlled FET switches integrated in the hosting substrate. The possibility of controlling the position of the band-gap, and implicitly the value of the effective dielectric constant along the line, for different combinations of the switches is demonstrated.

1. INTRODUCTION

Periodic or quasi-periodic structures are present in nature in various forms. Periodic configurations have also been employed in several fields of science, because they present some interesting characteristics that can not be achieved otherwise. These structures are formed by repeating a building block, called a unit cell, in one, two or three dimensions.

The main difference between the periodic and non-periodic structures is the possible presence of bandgaps in the former [1]. These

Corresponding author: L. Matekovits (ladislau.matekovits@polito.it).
† Also with Department of Electronic Engineering, Macquarie University, Sydney, NSW 2109, Australia

are the frequency intervals in which a wave cannot propagate. The propagation of waves (gravitational, telluric, electromagnetic, etc.) inside the infinitely extended structures can be represented by modes, which are specific configurations of the field topography that represent solutions of the homogeneous problem with appropriate boundary conditions. In the case of electromagnetic fields, the formulation is in terms of the Maxwell's equations.

The propagation of an electromagnetic wave in a periodic structure is described by the dispersion diagram (DD), which represents the variation of the wave number vs. frequency. The DD depends on the unit cell geometry and material properties within the unit cell. Once the dimensions of the unit cell and the materials are fixed the DD is fixed as well. This means the response of the system for given excitation is known, and is always the same. This is a serious constraint that leaves no possibility for adaptive features. Instead, if one can dynamically modify the media parameters inside the unit cell, it will create new opportunities that can be exploited in many applications.

Our interest is focused on surface waves, i.e., waves that travel along the discontinuities between different dielectrics. In the case of open, unbounded structures, like the microstrip structures considering here, the strongest discontinuity is usually encountered at the air-dielectric interface. The surface wave for these structures is partially in the dielectric and partially in the air. However, for more complicated microstrip structures, it could be in two, or even more different dielectrics. The phase velocity for microstrip can be expressed in terms of the effective dielectric constant, which takes into account the above mentioned phenomena, i.e., the wave propagation in a medium with different dielectric constants.

In the following, we will concentrate on the possibility of dynamically modifying the value of the effective dielectric constant inside a unit cell. This operation can be carried out in the same way for each unit cell, maintaining the periodic arrangement, or differently for different unit cells. In this second case the resulting structure will be quasi-periodic.

In the past, different mechanisms have been proposed, like electro-optic [2], magneto-dielectric [3], or use of gyrotropic slabs [4] for the purpose of changing the effective dielectric constant. Here a different, fully-electronic method is devised for these structures based on loading a microstrip. The microstrip loading is accomplished by selectively switching short-circuited metallic patches (see Fig. 1), which are positioned between the microstrip and the ground plane, locally changing the load on the microstrip line. FET switches directly integrated into the hosting substrate are used for the aforementioned

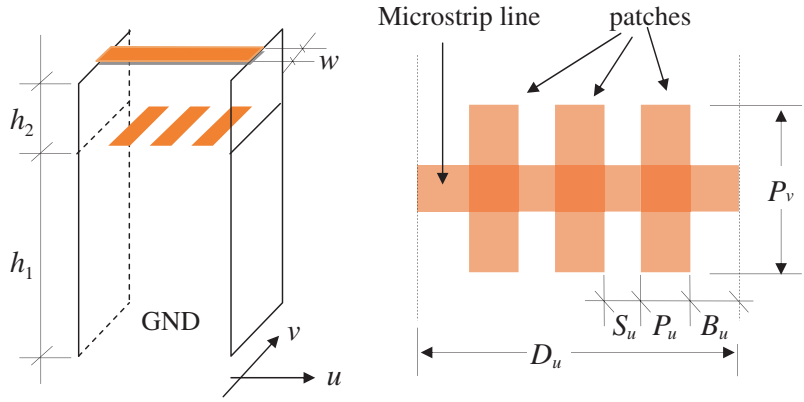

Figure 1. Unit cell: Configuration (left), top view (right).

purpose. When the active devices are not biased, they present high impedances, which can be modelled for precise characterization or simply assumed to be infinite. On the other hand, when they are biased their impedances are negligibly small and they act as short-circuits.

The use of diodes for similar purpose can be found in e.g., [5–7]. The main difference between the concepts in these works and what we are proposing here consists in the possibility of a finer tuning of the media parameters inside the unit cell. This is guaranteed by the large number of potentially short-circuited loads.

In the present version of our structure, shown in Fig. 1, the patches are positioned below the microstrip line but an exchanges of the position can also be considered. The patches in one cell can be of different size but here patches with the same dimensions are considered, without reducing the generality of the proposed method. To the end of each path two active devices are connected allowing them to be short-circuited to the ground in a selective way.

2. THE STRUCTURE

A unit cell with a length of $D_u = 340\mu$m in the u direction has been considered. The periodic structure is made out of two dielectric layers. A grounded GaAs substrate (L_1) with a thickness of $h_1 = 100\,\mu$m and a relative dielectric constant of $\varepsilon_{r1} = 12.9$ forms the base. Deposited on the GaAs is a second layer (L_2) with a thickness of $h_2 = 2\,\mu$m and a relative dielectric constant of $\varepsilon_{r2} = 6.5$. The selection of this stratification has been based on feasibility of fabrication with current technology.

The patches representing the passive reactive loads are located at the interface between L_1 and L_2. The microstrip line is positioned on the top of layer L_2. The patches and microstrip line, as well as the ground plane, are expected to be realized in gold of 1 µm thickness. The patches can be connected to the ground plane on the backside of the GaAs substrate with grounding vias.

We note that contrary to silicon (Si) which has high conductivity, GaAs is a relatively low-loss dielectric with relative dielectric constant of $\varepsilon_r = 12.9$. This high dielectric constant is also useful for miniaturization, since it reduces the resonant dimensions by roughly a factor of 3.

In particular, the unit cell with 3 identical patches, shown in Fig. 1, has been investigated. The patch dimensions are $P_u = 70\,\mu\text{m}$ and $P_v = 160\,\mu\text{m}$. They are positioned symmetrically with respect to the symmetry axes of the unit cell, and separated by a distance of $S_u = 20\,\mu\text{m}$. In this configuration, the distance B_u between the edge of a side patch and the unit cell boundary is equal to $45\,\mu\text{m}$. The microstrip line on the top of the structure has a width of $w = 60\,\mu\text{m}$.

Since $2 \times B_u \neq S_u$, the geometry has a double periodicity. This observation does not change the physics of the problem. It just represent a further degree of freedom, that may be exploited in the design.

From a manufacturing point of view, the thru-wafer via, or pin, which grounds the metal on the top to the backside of the wafer has dimensions of $63\,\mu\text{m} \times 93\,\mu\text{m}$. At least one of these is required in each unit cell. When fabricating, some space for the FET switches and the control lines to turn them off and on is also required. At this stage, the presence of these components has not been taken into account in the simulations.

3. EXTRACTION OF THE EFFECTIVE PARAMETERS

The propagation constant k in a periodic media assumes purely real values inside the band-gap, and is purely imaginary for a guided wave. For leaky waves, it takes a complex value, where the imaginary part is related to the phase variation along the structure, while the real part describes the leakage.

The knowledge of the imaginary part of k allows determination of the value of the effective dielectric constant ε_{eff} by the simple relation: $\varepsilon_{eff}(f) = (\frac{c\Im(k)}{2\pi f})^2$ where c is the speed of light in free space, f is the frequency and $\Im$ denotes imaginary part. Actually, this calculation gives the dispersion relation of the structure. In the following we

will present the computed values of k up to 150 GHz and analyze the behavior of ε_{eff}.

The determination of the propagation constant has been carried out by the method suggested in [8]. Two lines with different lengths have been considered: One has 6 unit cells ($6 \times 340 = 2040\,\mu$m long) and the second has 12 unit cells (4080 µm). The referenced method provides the propagation constant along the line, eliminating the effects of the discontinuity at the connector-line interface. Moreover, it makes no use of the line impedance, a useful observation for our case where the frequency band is very large. The characteristic impedance of the line varies with frequency, but its effect is not present due to the de-embedding method applied. The de-embedding method in [8] only requires that the characteristic impedances of the two lines be the same. This is fulfilled here, since the lines have the same width, and their variation with frequency is the same for the short and long cases.

These configurations have been analyzed for both the floating and grounded states of the patches. In the former case, all pathes are floating. This configuration will be denoted by (000), with clear reference to a three bit digital coding. The latter case (111) will be called fully short-circuited in the following. These configurations have been selected in order to verify the maximum variation of the response of the system.

The transmission coefficient between the two access ports has been computed using AWR's AXIEM electromagnetic software [9]. In all cases on the top of the structure an 500 µm air layer has been inserted, to guarantee more accurate results. The CAD model of the fully short-circuited pathes of the short line is presented in Fig. 2.

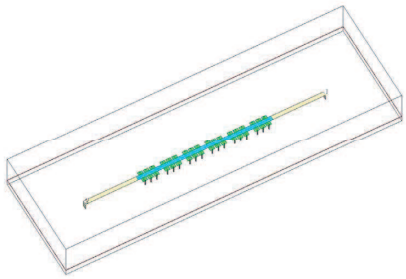

Figure 2. CAD model of line with fully short-circuited patches with 6 unit cells.

4. DISCUSSION OF THE NUMERICAL RESULTS

The dispersion diagram for both floating and fully short-circuited finite-dimension structures has been computed and are presented in Fig. 3. The corresponding values of the effective dielectric constants in the two cases are reported in Fig. 4. In both figures the first band-gaps are marked in gray. Note that the phase is π in the band-gaps.

As can be observed, the band-gap position can be shifted by as much as 80 GHz by shorting all patches inside the unit cell. This large variation in the position of the band-gap has been achieved by completely changing the propagation mechanism via the FET switches activating the shorting pins.

In order to check the tunability of the system, the transmission S_{21} parameters have also been computed for other two cases of biasing. In particular, the (101) and (010) configurations have been compared with the two extreme cases of (111) and (000). The results in Fig. 5 clearly demonstrates the tunability of the band-gap position by the proposed mechanism.

In the case of the fully short-circuited structure, the reactive loads switch from patches to loops, where a single loop is formed by one patch, its two shorting pins and the connection through the ground plane. The guiding structure becomes a helix, with a pitch angle of $\alpha = 1.2$ rad. Because of the high dielectric constant of the lower layer, the propagating electromagnetic wave is trapped inside the helix. The high dielectric constant will further reduce the phase velocity of the

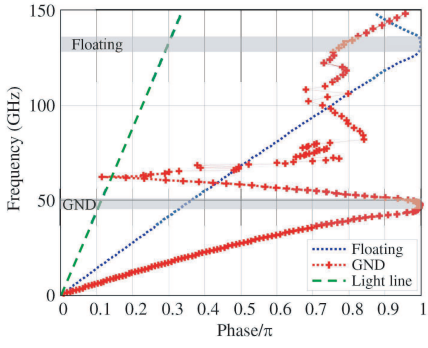

Figure 3. 1D dispersion diagram of a unit cell. The graph has been generated by extracting the propagation constant from the 6 and 12 cell configurations.

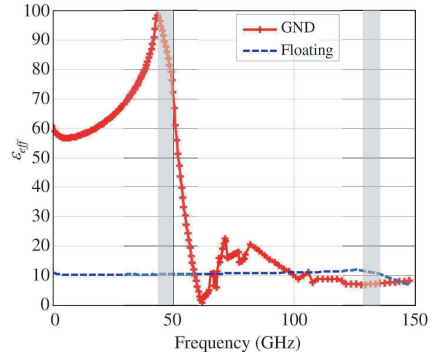

Figure 4. Comparison between the ε_{eff} for the floating and fully short-circuited cases for the considered unit cell.

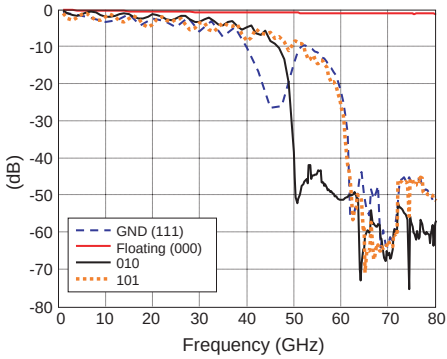

Figure 5. Variation of the band-gap position for different FET biasing combinations.

slow wave structure, amplifying the increase in the effective dielectric constant of the slow wave configuration.

The length of the resulting loop is $L_{loop} \approx 2(h_1 + D_u) = 880\,\mu\text{m}$. The resonance of such a loop occurs around the frequency $f_{r,loop} = \frac{c}{2L_{loop}\sqrt{12.9}} = 47.58\,\text{GHz}$. This value corresponds to the limit of the first stop band, which is also found from the full wave calculation results reported in Fig. 3.

The operational mode of the structure for the (111) and (101) biasing states are reported in Fig. 6. The equivalent helixes and the geometrical data needed for the characterisation of the propagation along the structure are explicitly indicated.

In the large frequency band we have considered, the operational mode of the helix continuously changes from normal to axial and vice-versa [10]. In the axial mode the coupling between adjacent loops is high, while in the normal mode operation the structure will interact in a more pronounced manner with the microstrip line. Leaky wave propagation starts when the second mode intersects the light line (see Fig. 3) allowing coupling between the guided and radiating waves [11]. The presence of the microstrip line and the ground plane will modify this radiation, but the leaky effect will still be present.

Furthermore, for the fully short-circuited case the ε_{eff} is not constant. At low frequencies, the behavior is dictated by the helix. This slow wave corresponds to a high effective dielectric constant of about 60 and eventually increases up to 100. In the second pass-band, it gets as high as 25. The variation of ε_{eff} in the pass band is due to the presence of the second periodicity, that characterized the structure as described in the previous section.

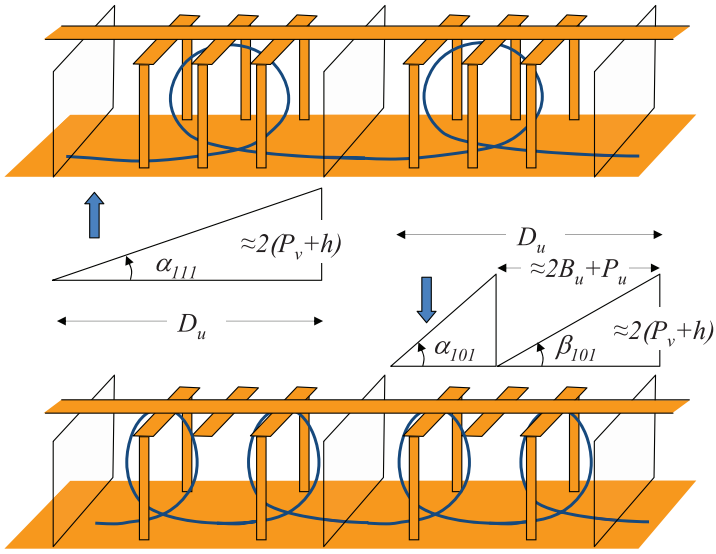

Figure 6. Equivalence between the geometries and propagation models for the 111 (top) and 101 (bottom) biasing states.

When the frequency further increases, the short circuited pathes act collectively as a ground plane with slots, allowing the electromagnetic field to penetrate into the layer L_1. The effect of the loops disappears and the field will concentrate in the upper layer (with $\varepsilon_r = 6.5$). The effective dielectric constant will be given by a weighted quantity between the dielectric constants of the three layers L_1, L_2 and air, and as expected, it takes lower values.

In the transition zone (from 60 to 80 GHz) the coupling between the two operational conditions can be observed for the fully grounded case.

For the floating case, the band gap starts at a higher frequency ($\approx$ 128 GHz), and the $\varepsilon_{eff}(f)$ is quite constant from very low frequencies up to the vicinity of the band gap. Its variation in the range from 10.27 to 11.5 corresponds to the expected behavior for a periodic structure.

5. CONCLUSION

The possibility of dynamically varying the position of a band-gap and consequently the value of the effective dielectric constant for 1D periodic structure in microstrip technology employing GaAs layers has been investigated numerically. The large variations of the considered

quantities have been obtained by completely changing the propagation conditions of the surface waves through combining the effects of periodic reactive loads with different working parameters of a helix-like slow wave structure. This change is obtained by dynamically controlled embedded FET switches. As well known, the limits of the band-gaps are related to resonances. The insertion of the loop as periodic load introduces a fundamental change in the operational conditions at about 80 GHz. Fine tuning and optimization of the geometries for a better control of the band-gap limits are in progress. Due to the several degrees of freedom, the structure can be optimized for different applications like steerable leaky-wave antennas, holographic antennas, adaptive radio frequency elements/software defined radio etc.. Extension to the 2D case is quite straightforward.

ACKNOWLEDGMENT

The authors are grateful to Murray Shattuck of AWR Corp. for his help and insight on simulating ε_{eff}.

This research was supported by a Marie Curie International Outgoing Fellowship within the 7th European Community Framework Programme.

REFERENCES

1. Brillouin, L., *Wave Propagation in Periodic Structures*, Dover, New York, 1953.
2. Linnik, L. A., "Novel devices and heterostructures based on modulated dielectric properties of materials," Ph.D. Thesis, University of Maryland College Park, 2001.
3. Mosallaei, H. and K. Sarabandi, "Magneto-dielectrics in electromagnetics: Concept and applications," *IEEE Trans. Antennas and Propagat.*, Vol. 52, No. 6, 1558–1567, 2004.
4. Huang, H., Y. Fan, B.-I. Wu, and J. A. Kong, "Tunable TE/TM wave splitter using a gyrotropic slab," *Progress In Electromagnetics Research*, PIER 85, 367–380, 2008.
5. Sievenpiper, D. F., "Forward and backward leaky wave radiation with large effective aperture from an electronically tunable textured surface," *IEEE Trans. Antennas and Propagat.*, Vol. 53, No. 1, Part 1, 236–247, 2005.
6. Bayatpur, F. and K. Sarabandi, "A tunable metamaterial frequency-selective surface with variable modes of operation,"

IEEE Trans. Microwave Theory and Techniques, Vol. 57, No. 6, 1433–1438, 2009.

7. Costa, F., A. Monorchio, S. Talarico, and F. M. Valeri, "An active high-impedance surface for low-profile tunable and steerable antennas," *IEEE Antennas and Wireless Propag. Let.*, Vol. 7, 676–680, 2008.
8. Reynoso-Hernndez, J. A., "Unified method of determining the complex propagation constant of reflecting and non-reflecting transmission lines," *IEEE Microwave and Wireless Components Let.*, Vol. 13, No. 8, 351–353, 2003.
9. http://web.awrcorp.com/
10. Watkins, D. A., *Topics in Electromagnetic Theory*, Chap. 2, John Wiley & Sons, Inc., New York, 1958.
11. Oliner, A. A. and D. R. Jackson, *Antenna Engineering Handbook*, J. Volakis (ed.), Ch. 11., Leaky-wave antennas, McGraw Hill, 2007.